DSS 15, 45, and 65 34-Meter High-Efficiency Antenna Radio Frequency Performance Enhancement by Tilt Added to the Subreflector During Elevation Angle Changes

M. S. Katow[1]
Ground Antenna and Facilities Engineering Section

The focusing adjustments of the subreflector of an az-el Cassegrainian antenna that use only linear motions have always ended in lateral offsets of the phase centers at the subreflector's focus points at focused positions, which have resulted in small gain losses. This article describes how lateral offsets at the two focus points were eliminated by tilting the subreflector, resulting in higher radio frequency (RF) efficiencies at all elevation angles rotated from the rigging angle.

I. Introduction

At the 45-deg elevation angle, the subreflector of the shaped Cassegrainian geometry radio frequency (RF) system of the 34-m high-efficiency antenna is focused for maximum RF gain. Any change in the elevation angle results in gravity loading displacements to the reflective RF surfaces and subsequent RF-gain loss due to the defocused condition of the Cassegrainian system.

An analysis method for determining the lateral and axial translations of the subreflector required to maintain its optimum focused position throughout the elevation angle range, without the ability to tilt the axis of the subreflector, was described in [1]. Lateral offsets of the phase centers existed at the optimum focused positions, which resulted in some RF-gain loss. This article describes how the addition of the tilting adjustment of the subreflector minimized the lateral offsets at the phase centers of the secondary reflector. This correction resulted in smaller RF-gain losses with elevation angle motions from the 45-deg rigging elevation angle.

II. Shaped Cassegrainian RF Geometry

The 34-m shaped Cassegrainian RF geometry, set at the 45-deg elevation angle, is illustrated in Fig. 1. Like a paraboloid, the inner rays reflected from the subreflector are moved outward, resulting in more uniform RF-amplitude distribution across the main reflector for increased RF efficiency. Also, the equivalent focal length, as defined in a paraboloid, increases from about 11.02 m

[1] M. S. Katow, who is assigned on contract to the Ground Antenna and Facilities Engineering Section, is an employee of Planning Research Corporation, McLean, Virginia.

(434 in.) at the center to about 11.81 m (465 in.) at the outer edge of the reflector.

Assuming a single phase center, the movement of the primary phase center of the main reflector during the elevation angle change was determined by best fitting a paraboloid to the gravity-loaded displacements of the reflector. This was done by using both the longer focal length to represent the major part of the reflector surface and the root mean square (rms) program [2] to best fit a paraboloid to the reflector distortions for the gravity loading changes from a 45-deg to a 90-deg elevation angle. The change is defined in Fig. 2. The gravity distortions of the reflector were computed using the IDEAS program [3] along with the displacement of the nodes supporting the subreflector on the quadrupod. The field-measured displacements[2] between the subreflector and its quadrupod supporting nodes with dial indicators were then added to the computed displacements to determine the deflected position of the subreflector for the same elevation angle change as for the reflector. The deflected position, as calculated by procedures described in the following paragraphs, is also shown in Fig. 2.

III. Subreflector Gravity Displacements

To measure the deflections of the subreflector's supporting and controlling mechanism, dial indicators were installed, using special fixtures, between the apex of the quadrupod and the top of the subreflector as shown in Fig. 3.[2] These dial indicators were set to 12.7 mm (0.5 in.) at 90-deg elevation, and the deflection figures were read as the antenna was rotated in elevation angle down from a 90-deg elevation angle to a 6-deg elevation angle. The readings are plotted in Fig. 4 for dial indicator No. 5.[3] The No. 1, No. 2, and No. 3 dial-indicator readings are shown in Fig. 5, where dial readings were also set at 12.7 mm (0.5 in.) at 90-deg elevation, and the displacements were read as the elevation angle was reduced to 6 deg from 90 deg.[3]

The computed displacements of the structural nodes of the quadrupod's apex for the gravity loading change from a 45-deg to a 90-deg elevation angle are given in Table 1. The computed displacements portion of the subreflector is shown in Fig. 6, where the deflections of the quadrupod's supporting nodes are resolved into the displaced position of the top surface of the subreflector and its central axis, with no displacements assumed in the subreflector's supporting and controlling mechanism. To account for the deflections in the subreflector's supporting and controlling mechanism, the dial indicator readings of Figs. 4 and 5 resolved into displacements are shown in Fig. 7 for a 90-deg elevation with the subreflector set on axis at a 45-deg elevation. The summed or total displacement of the subreflector is also shown in Fig. 2 for a 90-deg elevation with a 0 setting at a 45-deg elevation.

IV. Subreflector Supporting and Controlling Mechanism

The subreflector is supported by an assembly of three parallel plates in which the top plate is supported by three vertical jacks attached to the quadrupod. The top view of the vertical jacks' positions are shown in Fig. 8. The three plates are interconnected by slides and horizontal jacks to provide relative motion in the X- and Y-axes. Position indicating transducers parallel to the jacks provide a servo system where tables inserted in a microprocessor control the position of the jacks according to the elevation angle of the antenna.

V. Axial (Z)-Focus Curve Table

With the availability of field-measured Z-focus curve from the DSS 15 antenna, the focus-curves data from A. Freiley were used (Fig. 9).[4] The initially computed focus curve, designated as autofocus, was used in the DSS 15 servo controlling system. The measured focus curve indicated more deflection than was computed in the subreflector/reflector system and also showed an error in Z-positioning at a 45-deg elevation of −1.02 mm (−0.04 in.). A "measured" focus line is drawn through the experimental data. In order to develop an operating table for the microprocessor, it follows that:

$$Z = K\,(\sin(\text{elevation angle}) - \sin(\text{rigging el angle})) + \text{offset}$$

The fit of this curve with $K = 9.65$ mm (0.380 in.), with an offset of −1.0 mm (−0.039 in.), is shown by "X" points in Fig. 9. Reduced to table form, this curve when no tilting of the subreflector is done is shown in Table 2. Table 2 also delineates the curve with no offset, to be used when the zero-C focused position of the subreflector corresponds with the dial indicators.

[2] B. Parvin, "DSS-15 S/R Position Test," JPL IOM 3324-86-31 (internal document), Jet Propulsion Laboratory, Pasadena, California, April 21, 1986.

[3] Data by Ben Parvin.

[4] A. Freiley, "Preliminary Results of the 34M H.E. Antenna X-Band Performance Measurements at DSS-15," JPL IOM 3334-0885-023 (internal document), Jet Propulsion Laboratory, Pasadena, California, May 31, 1985.

VI. Subreflector Tilt and Y-Lateral Adjustments

Although the complex quadrupod assembly is modeled closely in the computing process, the deflections usually are larger than computed, as illustrated by Fig. 9. To address this problem, a 10-percent addition will be made to the computed and measured displacements of the subreflector. Also, to simplify the calculations, the assumption is made that the lateral adjusting jackscrews and the Z-axial jackscrews act on a plane on the same level as the top plate of the controlling mechanism. In other words, no interaction is assumed. This was thought to be consistent with the accuracy requirements.

Figure 10 delineates the total tilt and the Y-lateral adjustments required at a 90-deg elevation angle, starting from el = 45 deg, to focus the subreflector to the phase center of the primary RF feed horn and the primary focus of the best-fit paraboloid:

For el = 45 deg to el = 90 deg,

$$\text{tilt change} = \frac{3.101 - 2.298}{689.643} = 0.001164 \text{ rad}$$

For el = 45 deg to el = 90 deg,

$$\text{Y-travel} = -3.1001 + (31.75 \times 0.001164) = -3.064 \text{ cm}$$

When tilting the subreflector from el = 45 deg to 90 deg, the jackscrew length changes. Jackscrew No. 1 must be raised as follows:

$$0.001164 \times 1.194 \text{ m} = 1.390 \text{ mm } (0.055 \text{ in.})$$

Jackscrews No. 2 and No. 3 must be lowered as follows:

$$0.001164 \times -0.597 \text{ m} = -0.695 \text{ mm } (-0.0275 \text{ in.})$$

It turns out that the cosine function of the elevation angle accurately describes the tilting of the subreflector [1] from 0 deg to 90 deg. For jackscrew No. 1,

$$Z_1 = K_2 \, (\cos \, (\text{el}) - \cos \, (\text{rigging angle}))$$

$$+ \text{ Z-axial focus}$$

For jackscrews No. 2 and No. 3,

$$Z_{23} = \frac{-K_2 \, (\cos \, (\text{el}) - \cos \, (\text{rigging angle}))}{2}$$

$$+ \text{ Z-axial focus}$$

K_2 = total jack travel constant for 0-deg to 90-deg elevation angle change

$$= 1.390/\cos 45 \text{ deg} = 1.966$$

The summed jackscrew positions for tilt and axial focus corrections computed from the above equations are delineated in Tables 3 and 4. These table values can be incorporated in the microprocessor for controlling the subreflector jackscrews for axial and tilting adjustments during the elevation angle changes.

For the −3.064 cm (−1.206 in.) Y-lateral adjustment of the subreflector (Fig. 10) required to maintain focus at el = 90 deg after the elevation angle change from el = 45 deg, the total Y-lateral travel equals −3.064 cm (−1.206 in.) divided by cosine 45 deg or −4.333 cm (−1.706 in.), which equals Ky. It follows that the equation controlling the Y-lateral adjustment equals

$$Y = K_y \, (\cos \, (\text{El}) - \cos \, (45 \text{ deg}))$$

Finally, the Y-lateral positions shown in Table 5, computed from the above equation, can be incorporated in the microprocessor to control the Y-lateral motion of the subreflector.

VII. Conclusions

The described tables were installed first in the DSS 45 subreflector control system, and the measured efficiency data[5] are shown in Fig. 11, where the RF efficiencies ranged from about 67 to 70 percent at X-band.[6]

Although the measured RF efficiency change from a 45-deg elevation angle to a 10-deg elevation angle indicates only about a 3 percent drop, some field-checking focusing at the low angles should be done for possible improved RF-efficiency values. These field readings could then be used to upgrade the focusing tables in the subreflector's controller to enhance future operations required when higher RF frequencies are used.

---

[5] D. Bathker, "Data with Graham Baines, DSS-45," JPL IOM 3331-88-061 (internal document), Jet Propulsion Laboratory, Pasadena, California, June 30, 1988.

[6] Figure 11 reports measured efficiency according to existing standards (*DSN Radio Source List for Antenna Calibration*, JPL D-3801, Rev. B (internal document), Jet Propulsion Laboratory, Pasadena, California, September 25, 1987) and includes slight atmospheric extinction. The source flux and size standards within JPL D-3801, Rev. B are currently being revised such that the true peak antenna efficiency, sans atmosphere, is slightly over 75 percent. A revised *DSN Radio Source List* is being produced.

References

[1] R. D. Hughes and M. S. Katow, "Subreflector Focusing Techniques Applied to New DSS-15 and DSS-45 34-Meter Antennas," *TDA Progress Report 42-80*, vol. October–December 1984, Jet Propulsion Laboratory, Pasadena, California, pp. 83–90, February 15, 1985.

[2] M. S. Katow and L. W. Schmele, "Antenna Structures: Evaluation Techniques of Reflector Distortions," in *Supporting Research and Advanced Development, Space Programs Summary*, 37-40, vol. IV, Jet Propulsion Laboratory, Pasadena, California, pp. 176–184, April 15, 1967.

[3] R. Levy, "Optimization of Antenna Structure Design," *Eighth Conference on Electronic Computation*, ASCE, Houston, Texas, pp. 114–129, February 1983.

Table 1. Displacements of structural nodes of the quadrupod's apex

Node no.	Displacements		
	X, mm/in.	Y, mm/in.	Z, mm/in.
16131	0.23/0.009	17.70/0.697	−1.96/−0.077
16141	0.23/0.009	17.80/0.701	−1.96/−0.077
15130	−0.25/−0.010	17.70/0.697	−0.30/−0.012
15140	−0.25/−0.010	17.80/0.701	−0.30/−0.012

Table 2. Z-axial focus curve

Seq	Elevation angle, deg	sin, el	sin, el − sin, 45 deg	Z with K = 9.65 K = 0.38		Z with 1.02(−0.4) offset	
				mm	in.	mm	in.
1	0	0.0	−0.7071	−6.82	−0.269	−7.85	−0.309
2	10	0.1736	−0.5335	−5.16	−0.203	−6.17	−0.243
3	20	0.3420	−0.3651	−3.53	−0.139	−4.55	−0.179
4	30	0.5000	−0.2071	−2.01	−0.079	−3.02	−0.119
5	40	0.6428	−0.0643	−0.61	−0.024	−1.63	−0.064
6	45	0.7071	0.0	0.0	0.0	−1.02	−0.040
7	50	0.7660	0.0589	0.56	0.022	−0.46	−0.018
8	60	0.8660	0.1589	1.52	0.060	0.51	0.020
9	70	0.9397	0.2326	2.24	0.088	1.22	0.48
10	80	0.9848	0.2777	2.69	0.106	1.68	0.066
11	90	1.000	0.2929	2.82	0.111	1.80	0.71

Table 3. Jack 1 tilt corrections Z-axial focus

Seq	Elevation angle, deg	cos, el	cos, el − cos, 45 deg	(1) Tilt correction for jack no. 1		(2) Z−axial focus for no tilt	
				mm	in.	mm	in.
1	0	1.0	0.2929	−0.58	−0.023	−6.83	−0.269
2	10	0.9848	0.2777	−0.53	−0.021	−5.16	−0.203
3	20	0.9397	0.2326	−0.46	−0.018	−3.53	−0.139
4	30	0.8660	0.1589	−0.30	−0.012	−2.01	−0.079
5	40	0.7660	0.0589	−0.13	−0.005	−0.61	−0.024
6	45	0.7071	0.0	0.0	0.0	0.0	0.0
7	50	0.6428	0.0643	0.13	0.005	0.56	0.022
8	60	0.5000	−0.2071	0.41	0.016	1.52	0.060
9	70	0.3420	−0.3651	0.71	0.028	2.24	0.088
10	80	0.1736	−0.5335	1.07	0.042	2.69	0.106
11	90	0.0	−0.7071	1.40	0.055	2.82	0.111

Table 4. Focused jack positions

Seq	Elevation angle, deg	(3)[a] Jack no. 1 Z-position		(4)[b] Jacks no. 2 and no. 3 Z-position	
		mm	in.	mm	in.
1	0	−7.41	−0.292	−6.55	−0.258
2	10	−5.69	−0.224	−4.90	−0.193
3	20	−3.99	−0.157	−3.30	−0.130
4	30	−2.31	−0.091	−0.85	−0.073
5	40	−0.74	−0.029	−0.53	−0.021
6	45	0.0	0.0	0.0	0.0
7	50	0.69	0.027	0.51	0.020
8	60	1.93	0.076	1.32	0.052
9	70	2.95	0.116	1.88	0.074
10	80	3.76	0.148	2.16	0.085
11	90	4.22	0.166	3.52	0.139

[a] Column (3) = column (1) + column (2).

[b] Column (4) = $-\frac{\text{column(1)}}{2}$ + column (2).

Table 5. Y-lateral adjustments

Seq	Elevation, deg	cos, el	(a) cos, el − cos, el_{45}	(a) × 1.706 = Y-lateral position
1	0	1.0	0.2929	0.500
2	15	0.9659	0.2588	0.442
3	30	0.8660	0.1589	0.159
4	45	0.7071	0.0	0.0
5	60	0.5000	−0.2071	−0.207
6	75	0.2588	−0.4483	−0.765
7	90	0.0	−0.7071	−1.206

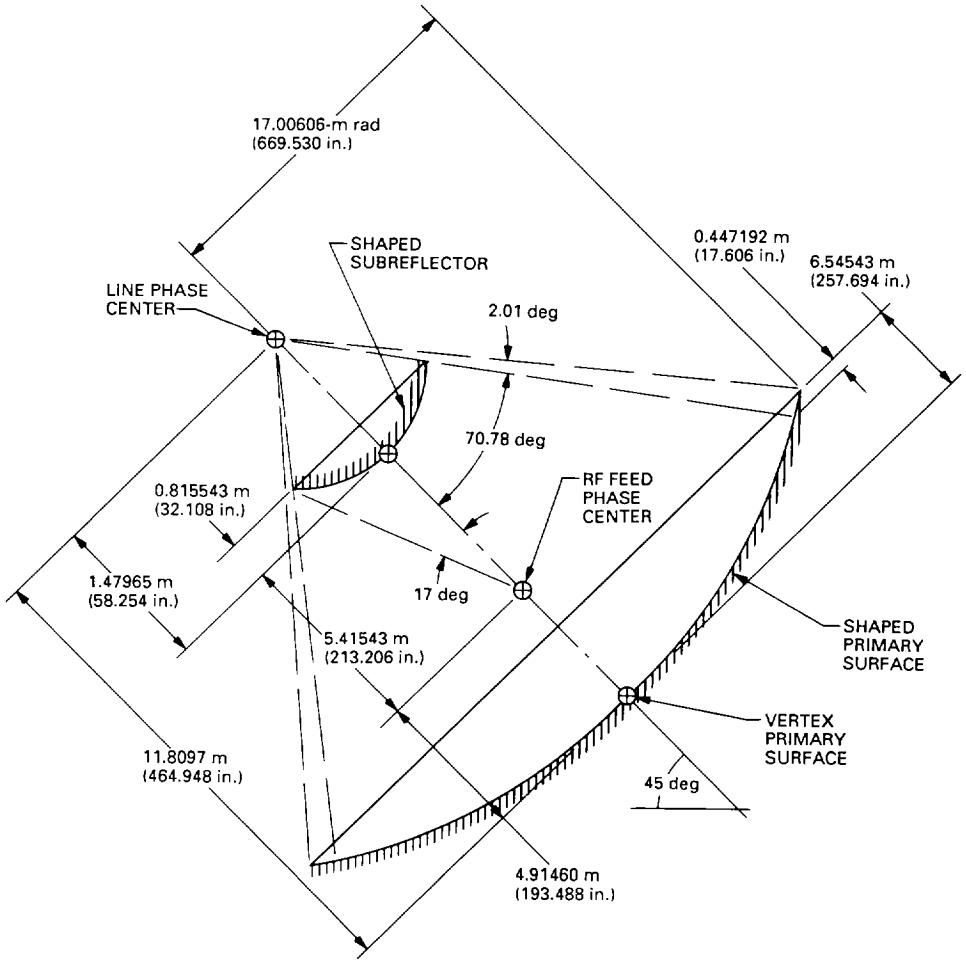

Fig. 1. The 34-m shaped Cassegrainian RF geometry at 45-deg elevation angle.

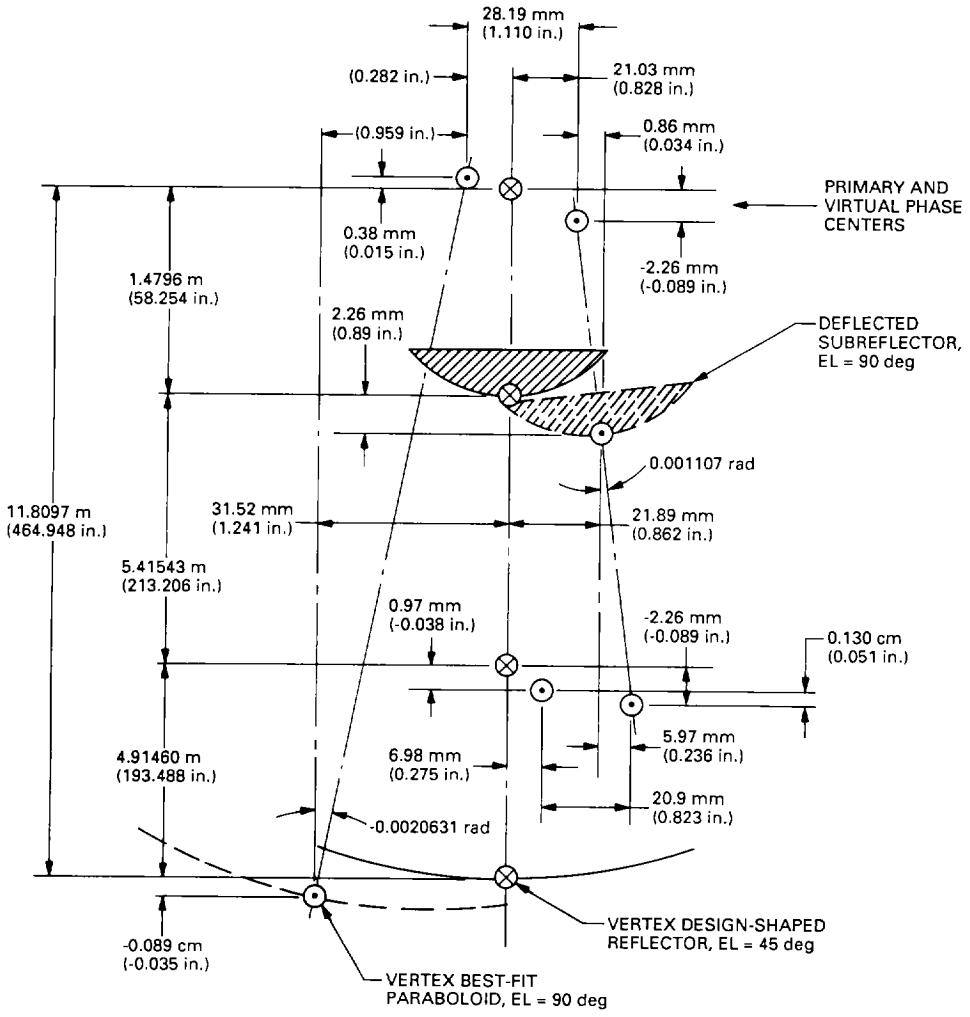

Fig. 2. Cassegrainian displacements at el = 90 deg with surfaces set at el = 45 deg.

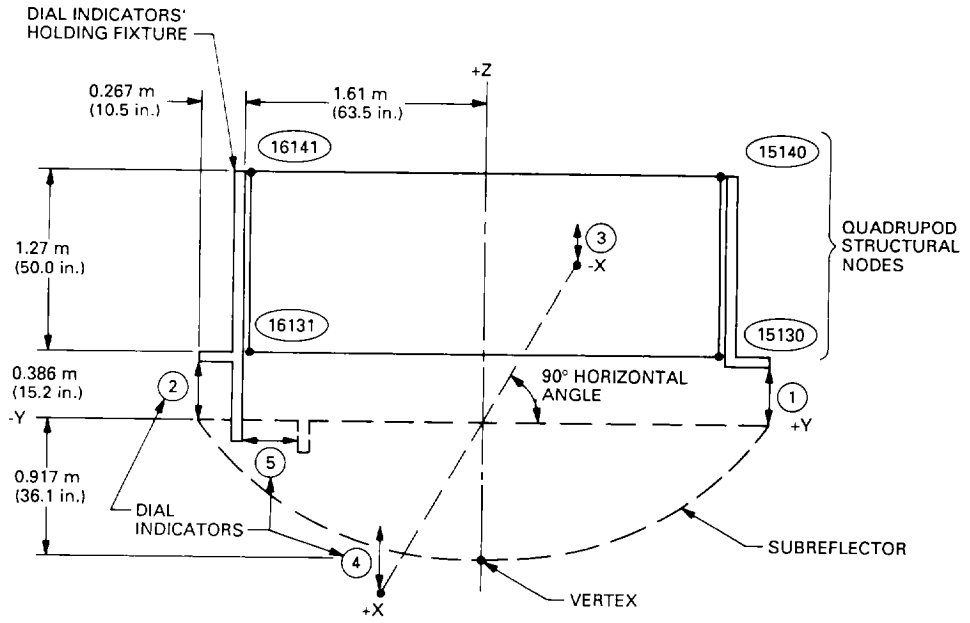

Fig. 3. Dial indicator locations.

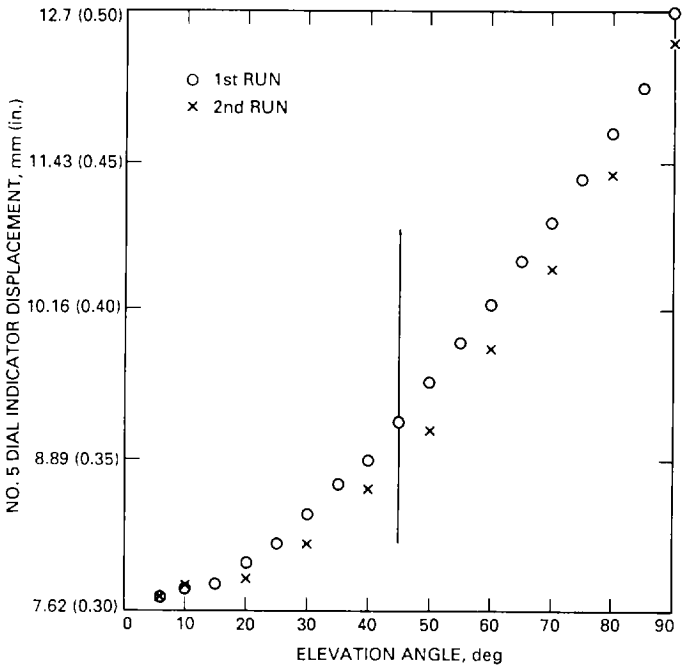

Fig. 4. The 34-m az-el subreflector field deflections from apex, No. 5 dial indicator (shown in Fig. 3), lateral displacements.

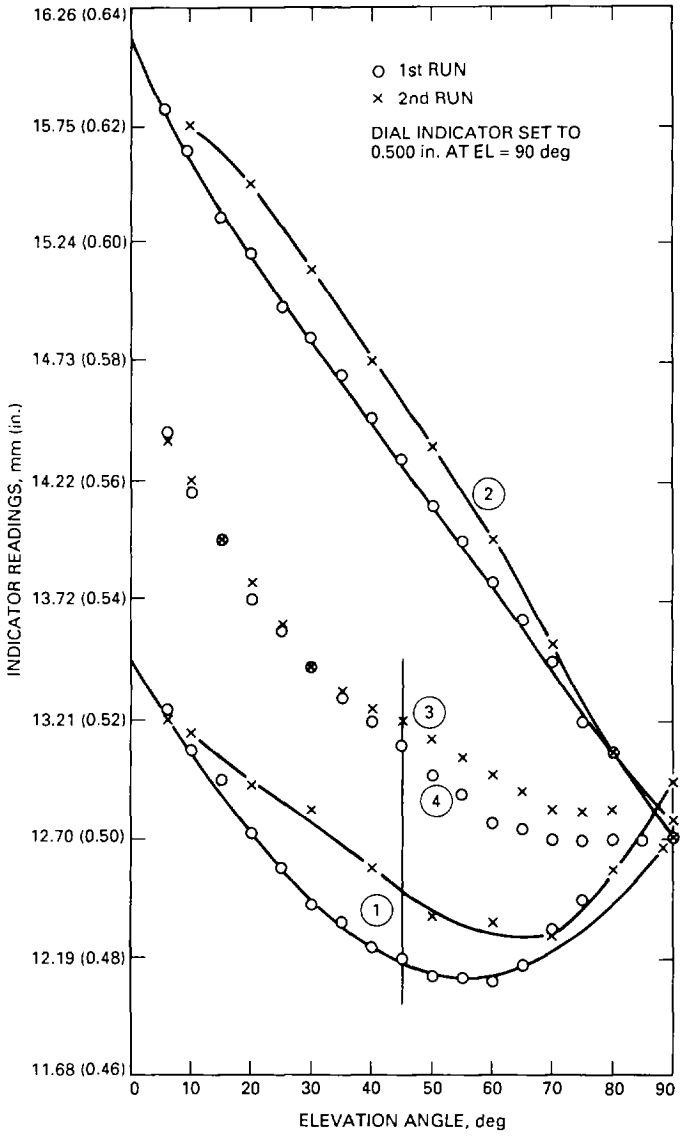

Fig. 5. The 34-m az-el subreflector field deflections from apex, No. 1, No. 2, No. 3, and No. 4 dial indicators (shown in Fig. 3).

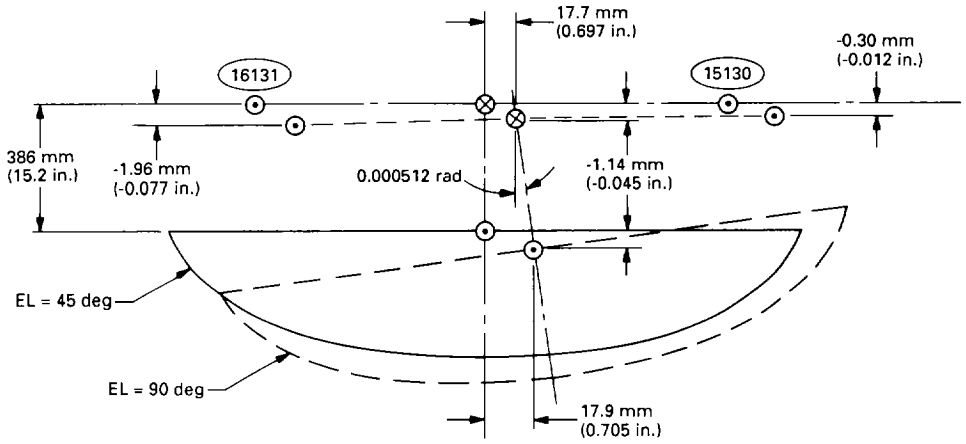

Fig. 6. Computed displacements of subreflector at el = 90 deg, set at 45 deg.

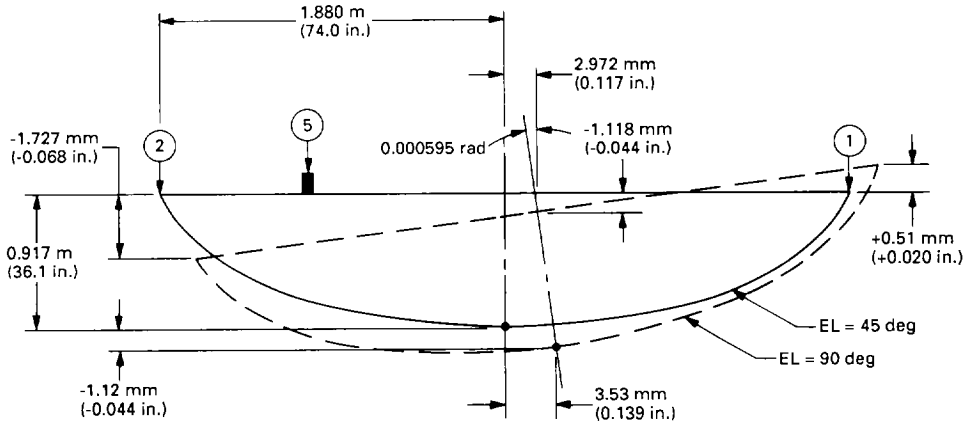

Fig. 7. Dial-indicated displacements of subreflector at el = 90 deg, set at 45 deg.

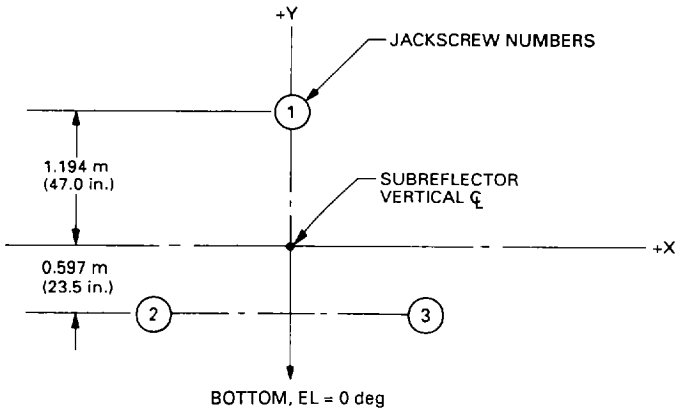

Fig. 8. X-Y jackscrew locations on quadrupod.

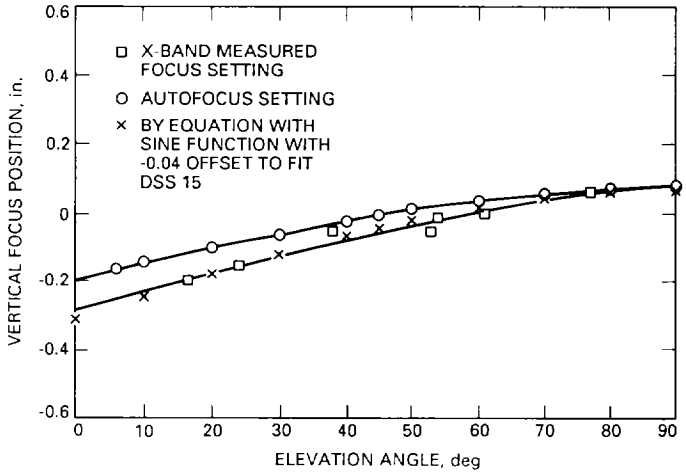

Fig. 9. The 34-m field data, DSS 15.

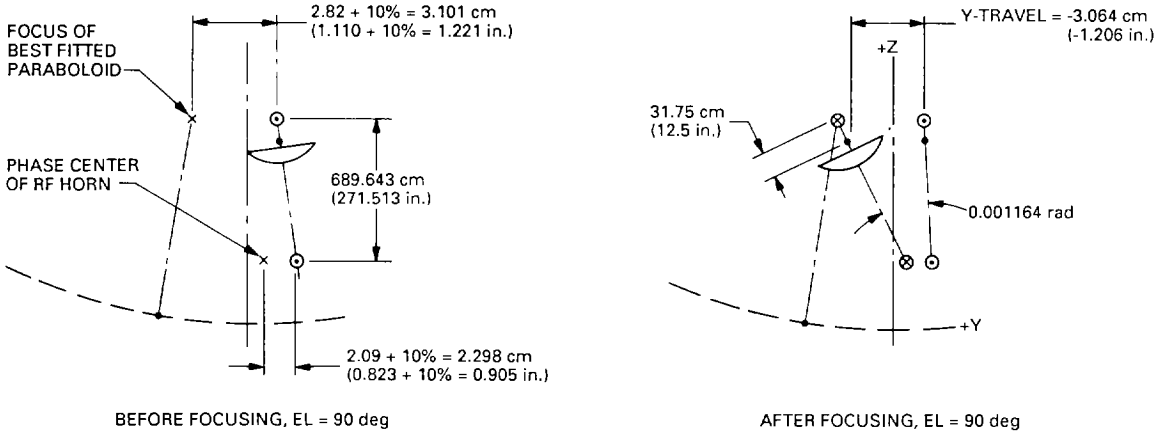

Fig. 10. Subreflector lateral and tilt focusing adjustments, el = 45 deg to el = 90 deg.

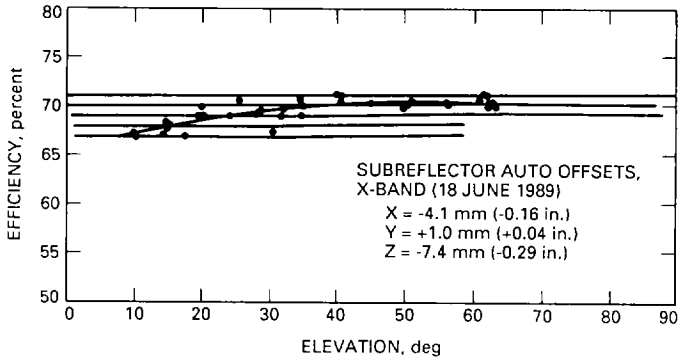

Fig. 11. DSS 45 measured efficiency.